Supplementary Information: Neurons in macaque Area V4 are tuned for complex spatio-temporal patterns

Anirvan S. Nandy[1], Jude F. Mitchell[1,3], Monika P. Jadi[2] & John H. Reynolds[1]

[1]Systems & [2]Computational Neurobiology Laboratories

The Salk Institute for Biological Studies, La Jolla, CA 92037

[3]Current address: Dept. of Brain & Cognitive Sciences, University of Rochester,

Rochester, NY 14627

Corresponding author: A.S.N. (nandy@snl.salk.edu)

Supplementary Figure-1 NANDY

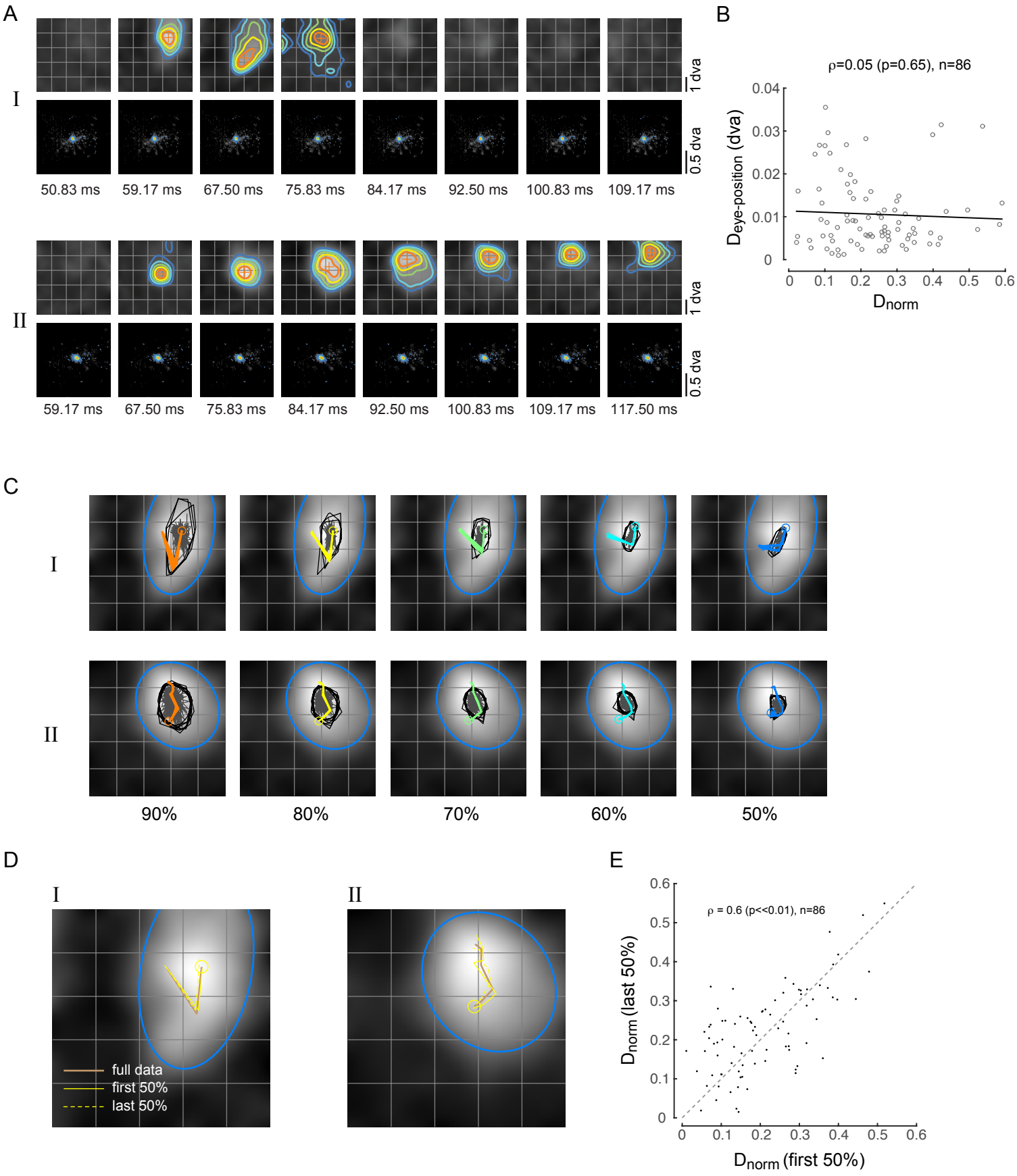

Supplementary Figure-2 NANDY

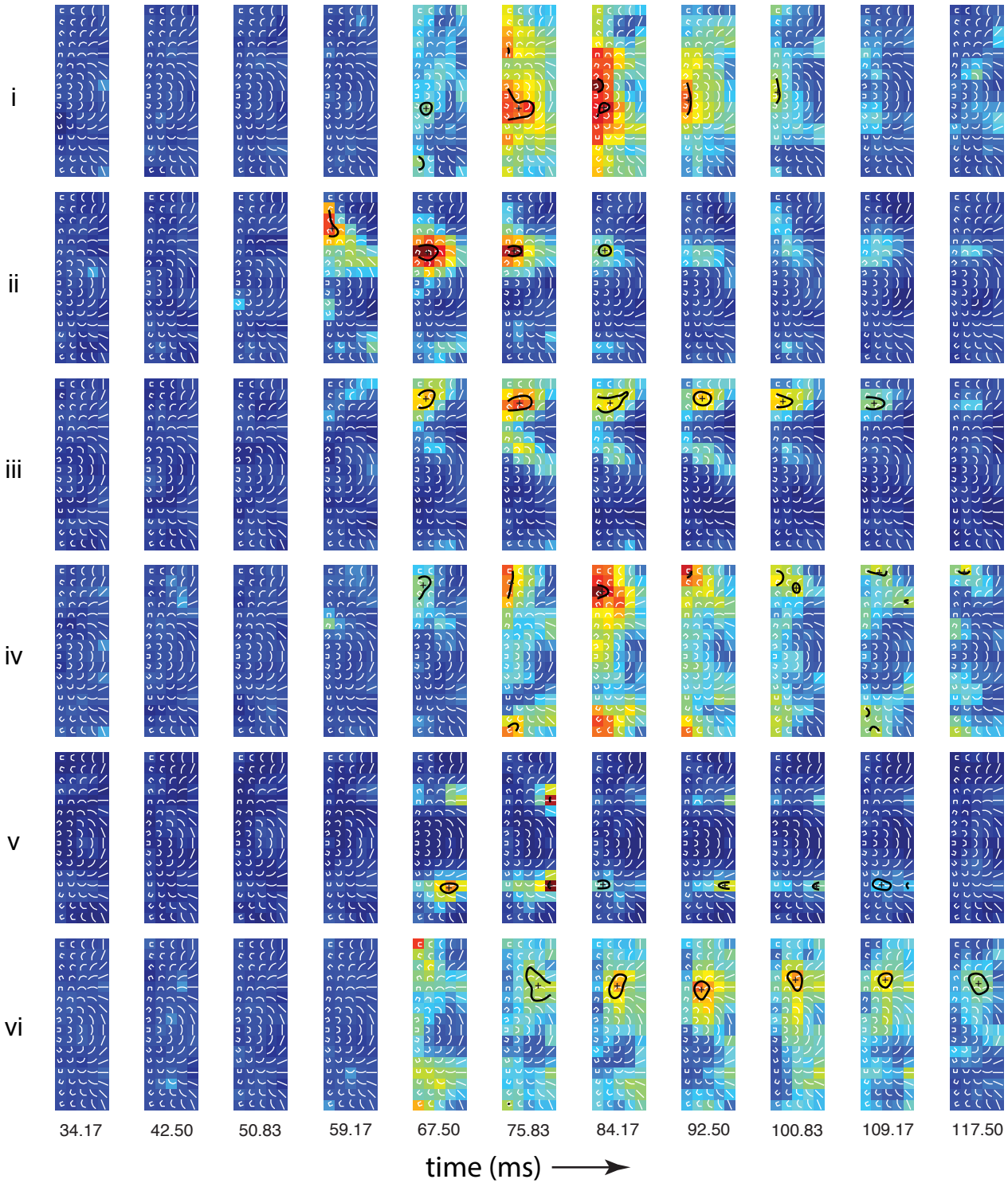

Supplementary Figure-3 NANDY

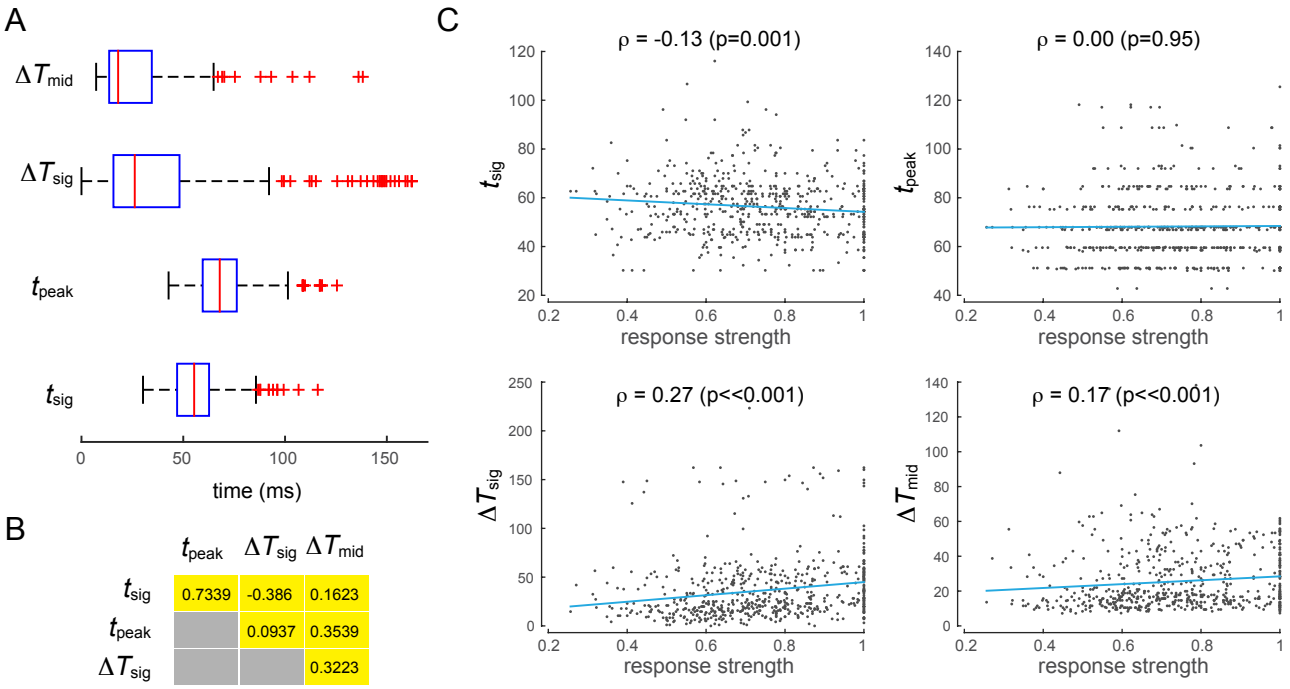

B

	t_{peak}	ΔT_{sig}	ΔT_{mid}
t_{sig}	0.7339	-0.386	0.1623
t_{peak}		0.0937	0.3539
ΔT_{sig}			0.3223

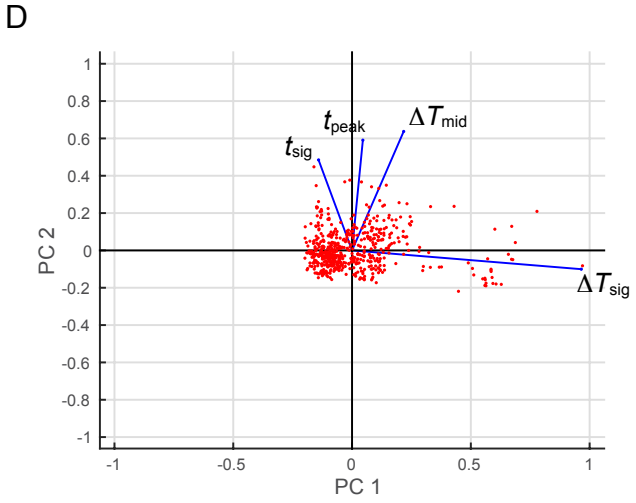

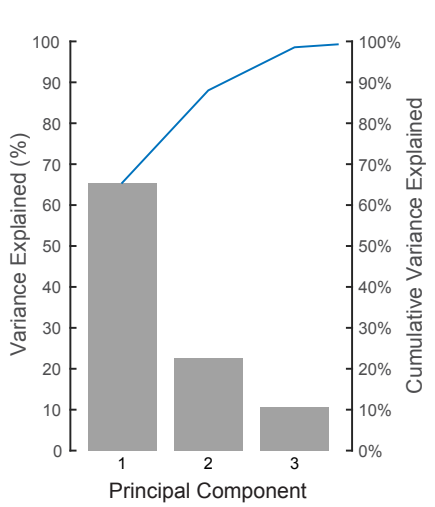

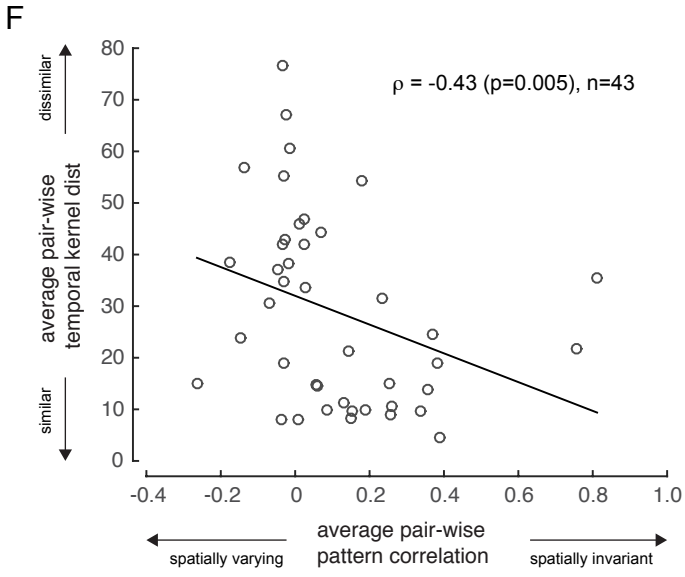

Supplementary Figure-4 NANDY

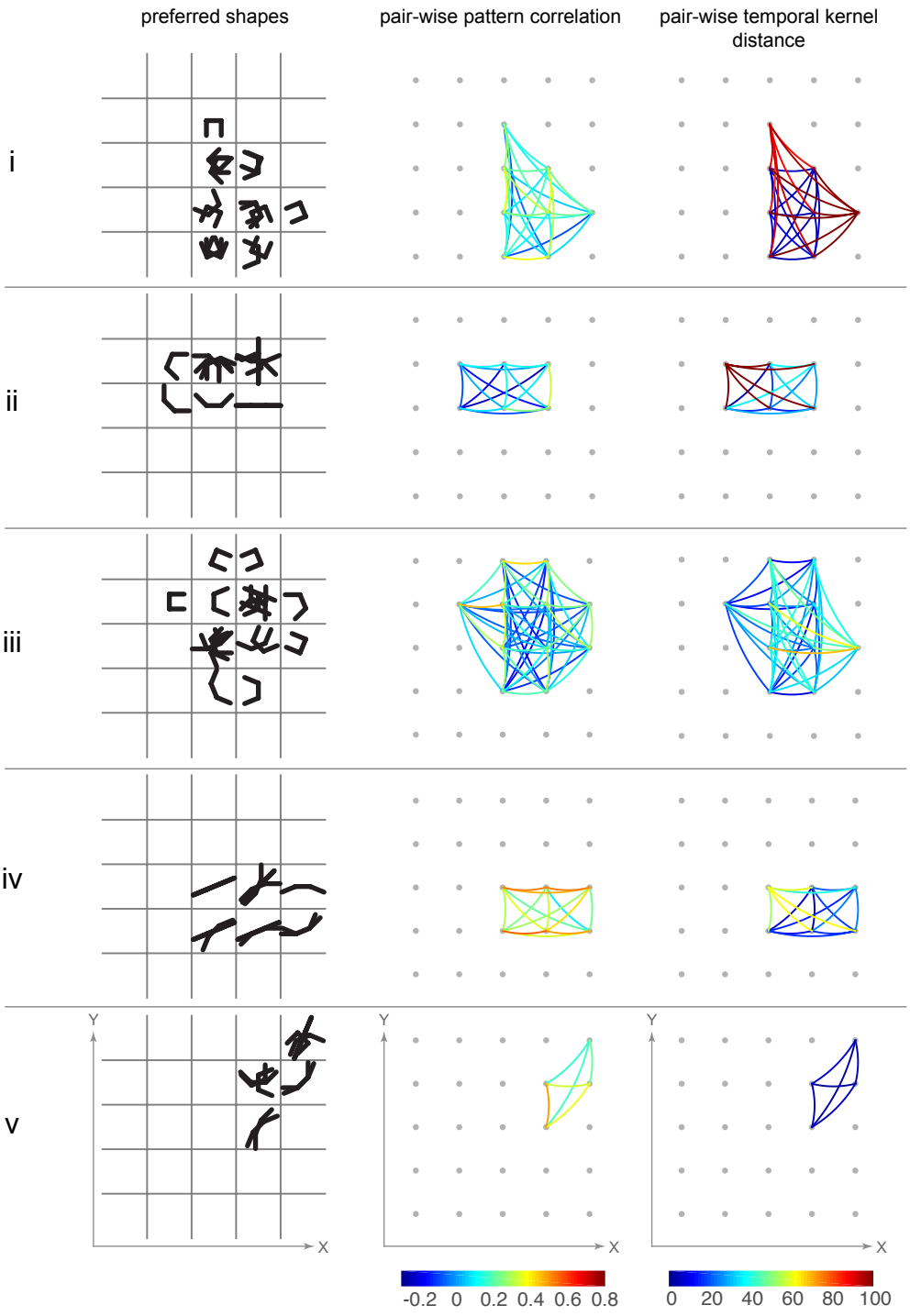

Supplementary Figure-5 NANDY

A

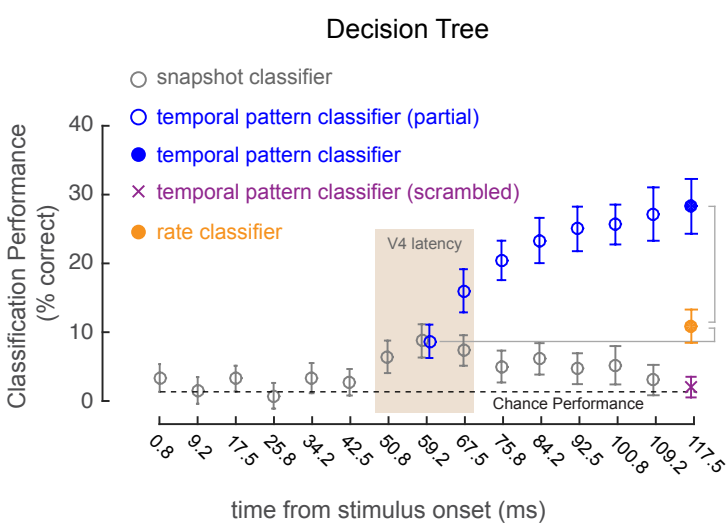

B

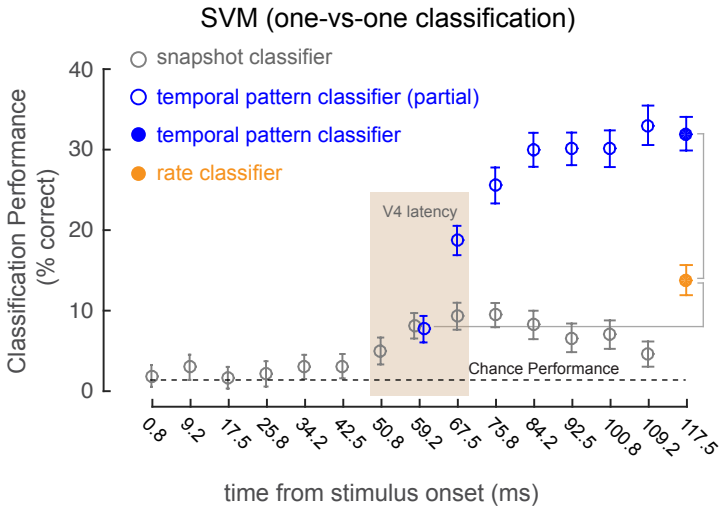

Supplementary Figure-6 NANDY

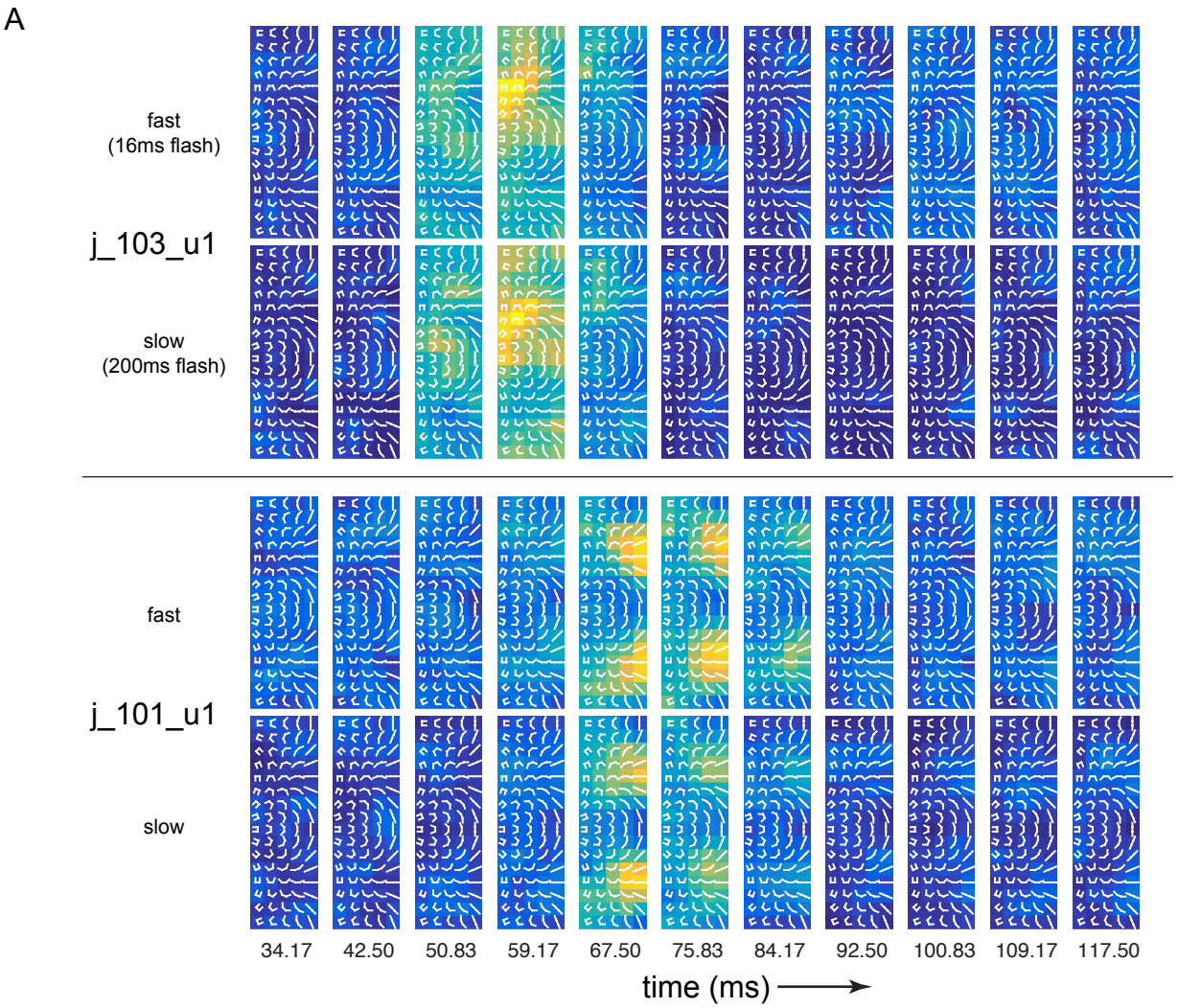

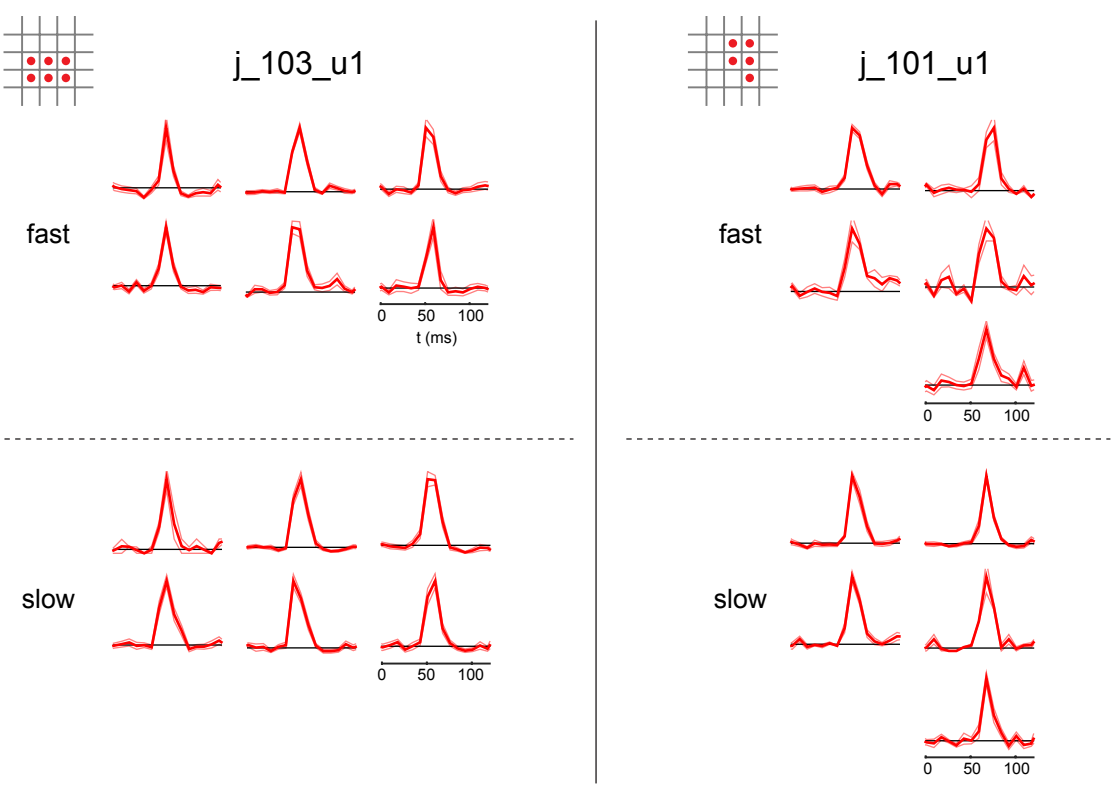

SUPPLEMENTARY FIGURE LEGENDS

Supp Fig 1. Independence of fine-scale STRFs from fixational eye-movements and the stability of spatial trajectories. **Related to Figs 2-3.** (**A**) For 2 example neurons (neurons I & II in Fig 2): *Upper panels*, temporal evolution of fine-scale STRFs (same format as in Fig 2, lower panels). *Lower panels*, corresponding distribution of eye-positions. dva: degree of visual angle. (**B**) Scatter-plot of the maximum spatial excursion of STRF trajectories (D_{norm}, Fig 3) versus the maximum dispersion of eye-position ($D_{\text{eye-position}}$; calculated from the same time-bins used to calculate D_{norm}) show no correlation between the two quantities. (**C**) Stability of spatial trajectories across response levels: spatial trajectories are shown for the same example neurons in **A** at 5 response levels (90, 80, 70, 60 and 50% of local peak). Same format as in Fig 3A. (**D**) Stability of spatial trajectories over measurement duration: spatial trajectories are shown for the same two example neurons in **A** and **B** for the full data set, the first 50% of trials and the last 50% of trials. (**E**) The normalized spatial excursions of the trajectories, D_{norm}**,** for the first 50% of trials versus the last 50% of trials are plotted for the population of neurons. The two measurements are highly correlated ($\rho = 0.6, p \ll 0.01$)**.**

Supp Fig 2. **Coarse-scale STRFs**. **Related to Fig 4**. Neuronal response maps to the set of composite shapes (overlaid in white) are shown for six example neurons (rows) at their respective most responsive spatial location on the 5x5 response grid. Response contours at 90% of local peak are superimposed for all significant time bins (see Experimental Procedures). '+' signs depict the centroids of the contour lines.

Supp Fig 3. **Principal components analysis on the temporal response profiles**. **Related to Fig 5**. (**A**) The box-plots show the distribution of the four parameters, t_{sig}, ΔT_{sig}, t_{peak} and ΔT_{mid} (Fig 5) that were extracted from the temporal response profiles at each spatially significant location for all neurons in the population. On each box, the central mark is the median; the edges of the box are the 25th and 75th percentiles. (**B**) Correlation (Spearman's ρ) among the four parameters in **A**. t_{sig} are t_{peak} are strongly positively correlated. t_{sig} and ΔT_{sig} are negatively correlated. (**C**) Scatter-plot of the four parameters in **A** versus the normalized peak response at the corresponding spatial location in the receptive field. The responses were normalized by each neuron's maximum response across all spatial locations. t_{sig} has weak negative correlation with response strength. ΔT_{sig} and ΔT_{mid} respectively show modest and weak positive correlation with response strength. There is no correlation between t_{peak} and response strength. (**D**) Each dot is a projection of points in the 4D space (defined by the parameters in **A**) onto the 2D plane defined by the first two principal components. The four vectors (blue) indicate how each of the four parameters contributes to the two principal components. The projections of the vectors onto the two principal component axes are the coefficients of the principal components. (**E**) The variance explained by the top 3 principal components in the space defined by the 4 parameters in **A**, and the cumulative variance explained. (**F**) The average pair-wise temporal kernel distance is plotted against the average pair-wise pattern correlation (same format as in Fig 5C) for the subset of neurons whose D_{norm} values are in the top 50$^{\text{th}}$ percentile (n=43). There is a significant negative correlation (Spearman's $\rho = -0.43, p = 0.005$) between the two quantities.

Supp Fig 4. **Preferred shapes, pair-wise pattern correlation and pair-wise temporal kernel distance**. **Related to Fig 5**. Preferred shapes at different spatial locations (left column), response pattern correlation between pairs of spatial locations (middle column) and temporal kernel distance between pairs of spatial locations (right column) are shown for 5 example units (rows). *Left column*: the location-specific shape or set of shapes to which the neuron responded preferentially, at all spatially significant locations. Shapes are spatially superimposed at each grid location. *Middle column*: The undirected graphs show the pattern correlation (Pearson correlation between the response patterns to the set of composite shapes at a pair of spatial locations, see Experimental Procedures) for all possible location pairs with significant response. Warmer colors indicate that the location pairs have similar shape selectivity, while cooler colors indicate dissimilar shape selectivity. *Right column*: The undirected graphs show the distance, D, between pairs of temporal kernels (see Experimental Procedures) for all possible location pairs with significant

response. Coolers colors indicate that location pairs have similar temporal response patterns, while warmer colors indicate dissimilar temporal response patterns. The examples are arranged such that the ones near the top are spatially varying in their shape selectivity, while those near the bottom are spatially invariant. The pair-wise pattern correlations for the neurons with spatially varying tuning (e.g. neurons i and ii) are dominated by low-values (cold colors), while their pair-wise temporal kernel distance are dominated by high values (warm colors). The reverse pattern is seen for neurons with spatially invariant tuning (e.g. neurons iv and v).

Supp Fig 5. **Related to Fig 6**. **A population code of temporal response patterns far outperforms one with only rate information**. (**A**) 72-way shape classification performance for different categories of population codes using decision tree classifiers. Same format as in Fig 6B. Symbols are mean ± std. dev. classification performance for 10-fold cross-validated classification. (**B**) Shape classification for the different categories of population codes using support vector machine (SVM) classifiers with a linear kernel. Since SVM does not directly support multi-way classification, a one-versus-one (OVO) approach was used. Symbols are mean ± std. dev. classification performance for 10-fold cross-validated classification.

Supp Fig 6. **Related to Figs 2-4**. **Temporal response patterns are independent of stimulus duration**. (**A**) Neuronal response maps for two example neurons (rows), to the set of composite stimuli (overlaid in white) at their maximally responsive spatial location for fast (16ms duration; upper panels) and slow (200ms; lower panels) stimulus presentations. The temporal response patterns are virtually identical. (**B**) Normalized temporal response profiles (mean ± s.e.m.) for the same example neurons in **A**, at all spatially significant response locations on the 5x5 response grid (locations marked with red dots).